

## Theory of vertical and lateral Stark shifts of excitons in quantum dots

M. Sabathil\*, S. Hackenbuchner, S. Birner, J. A. Majewski, P. Vogl, and J. J. Finley

Walter Schottky Institut, Technische Universität München, Am Coulombwall, 85748 Garching, Germany

Received 30 September 2002, accepted 2 December 2002

Published online 23 June 2003

PACS 68.65.Hb, 73.21.La, 78.67.Hc

We present charge self-consistent 8-band  $k \cdot p$  calculations of the quantum confined Stark shift of excitons for self-assembled buried InGaAs quantum dots. Many different shapes and alloy profiles of the dots have been systematically studied. We predict the Stark shift of excitons for simultaneously applied vertical and lateral electric fields, taking into account realistic alloy profiles in the quantum dot. The study of the Stark shift of neutral excitons and in both vertical and lateral electric field directions provides a wealth of information about the coupling of the exciton to external perturbations. We show that the combination of lateral and vertical electric fields provides a particularly sensitive probe of the dot shape and alloy composition.

**1 Introduction** The shape and alloy composition of self-assembled InGaAs quantum dots that are buried beneath a cap layer of GaAs is currently of great interest but still poorly understood. There are several direct experimental methods such as STM [1, 2], TEM [3], or X-ray diffraction [4] that provide some information about the composition of the quantum dots. However, all of these techniques have the drawback of either being destructive or being limited to dots on the surface that differ from buried quantum dots (QD). By contrast, the recent development of single dot spectroscopy [5–7] allows one to examine the optical properties of individual quantum dots under the influence of external perturbations such as electric or magnetic fields [8–13]. The dependence of the optical and electronic properties on these external fields provides an important albeit indirect probe of the shape and alloy composition of the quantum dot [7]. This situation calls for the development of a reliable, quantitative theoretical model for the electronic properties of QD of any given shape and alloy profile, in order to be able to link measured exciton energies or relative transition intensities of single QD with their shape and composition.

In this work we present systematic predictions of the bias dependence of the electronic structure of self-assembled quantum dots for a wide variety of dot shapes, alloy profiles and show that the combined effect of applied and (piezoelectric) internal electric fields yields detailed information about shape and composition profiles. Several approaches have been published for the calculation of electronic properties of quantum dots, most prominently atomistic calculations [14, 15], as well as  $k \cdot p$  calculations [16, 17]. However, fully self-consistent computations of the total crystal energy, including the long range Coulomb fields for large systems are still out of reach. The neglect of piezoelectric and applied electric fields in current atomistic approaches such as empirical pseudopotential [14] or empirical tight-binding [15] methods does not allow one to study the response of QDs to applied fields. In addition, the detailed alloy profile is unknown even on a mesoscopic scale and even more so on an atomistic scale. In this work we therefore chose a multiband- $k \cdot p$  Schrödinger–Poisson approach that takes into account the Coulomb

\* Corresponding author: e-mail: sabathil@wsi.tu-muenchen.de, Phone: +49 89 289 12762

interaction between confined electrons and holes, as well as the applied and induced piezoelectric fields fully self consistently. Besides, this computationally efficient scheme allows us to systematically study hundreds of configurations and biases. We obtain a detailed understanding of the excitonic properties in QD as a function of lateral as well as vertical electric fields. We show that these field dependent excitonic transition energies provide unambiguous information about the shape and alloy composition of the QD in all three dimensions, including the vertical and lateral variations of the Indium concentration in the InGaAs QD.

**2 Theory** The present calculations have been carried out with the device simulator `nextnano`<sup>3</sup> [16]. Based on single particle eigenstates obtained from the solution of an 8-band  $k \cdot p$  Hamiltonian, the exciton energy is calculate self-consistently within the Hartree approximation. Assuming a separable exciton wave function, the Coulomb interaction between electron and hole is calculated by iteratively solving the Poisson and Schrödinger equation for each particle taking into account external and internal potentials including image charges due to the variation of the dielectric constant. The equations are solved within a finite differences scheme on an inhomogeneous grid with 1 nm grid spacing inside the quantum dot resulting in about  $3 \times 10^5$  grid points. The strain is calculated by minimizing the total elastic energy [18], including the wetting layer and a sufficiently large GaAs substrate and cap volumes, in order to minimize artefacts from boundaries. The resulting strain-induced band deformations and piezoelectric charges are fully taken into account in the above self-consistent cycle. In this way we have calculated exciton transition energies for various In(Ga)As dot shapes and alloy profiles under the influence of vertically and laterally applied electric fields.

**3 Quantum dot shapes and alloy profiles** The simulated structure consists of a 20 nm thick GaAs substrate, a 1 nm wetting layer with an indium content of 50% and the quantum dot with an In concentration that varies from 50% to 100%. The dot is capped by a GaAs layer. We have examined two classes of QD shapes that have been discussed in the literature [7, 14, 17], lens-shaped and truncated pyramidal (“obelisk”) dots namely as shown in Fig. 1. The height of the QD has been systematically varied from 3 to 5 nm and the base width from 15 to 25 nm, respectively. These values lie within the range of experimentally estimated dot sizes. In addition, we considered two types of alloy profiles, a simple linear and an angular profile that is. In the latter case, the indium concentration varies with the polar angle relative to the center axis of the dot, as shown in Fig. 2. This profile is supported by STM measurements and by theoretical models [2] of the growth process and leads to an inverted pyramid of high indium content inside the quantum dot (Fig. 2). The most important feature of this alloy profile is the fact that it produces a vertical and a lateral variation of the indium concentration which has been neglected so far.

**4 Lateral and vertical Stark shift** The change of the single exciton transition energy in response to an applied bias, i.e. the quantum-confined Stark shift, is a widely studied effect in QD [5, 7, 8–13]. So far, theoretical and experimental work focused solely on the effect of vertical electric fields applied along the QD growth axis. However, fabrication of four terminal photodiode structures that incorporate a pair of implanted top contacts in a lateral split-gate geometry, in addition to a vertical MIS photodiode structure, would enable the simultaneous application of vertical and lateral electric fields. Devices incorporating such lateral capacitor concepts have already been realized in the II–VI system [19], enabling application of laterally orientated electric fields in the range  $\pm 20$  kV/cm. Our calculations show that the analysis of the response of the exciton wave function to simultaneously applied lateral and vertical electric fields provides a whole new inside into the structure and the composition of the QD.

We have studied three different lateral field directions in the present calculations as shown in Fig. 1. Note that the strain and the resulting piezoelectric charges lead to an asymmetry which is reflected in the different Stark shifts for the various directions.

We have calculated the ground state exciton energy as a function of the vertical ( $F_v$ ) and lateral ( $F_l$ ) electric field and have fit the resulting Stark curves to a biquadratic form,

$$E(F_l, F_v) = E_0 + p_l F_l + p_v F_v + \chi_l F_l^2 + \chi_v F_v^2 + \chi_{lv} F_l F_v .$$

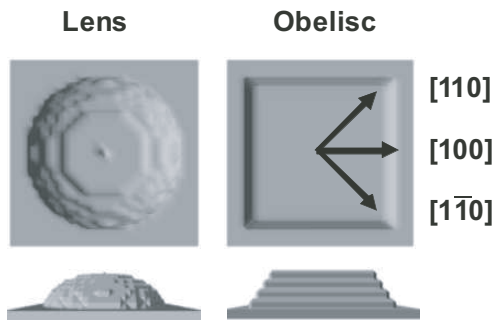


**Fig. 1** Two types of quantum dot shapes considered in this work: lens and obelisc shapes. The height and base width of these dots are varied between 3 to 5 and 15 to 25 nm, respectively. The directions of the lateral electric fields that are taken into account are indicated.

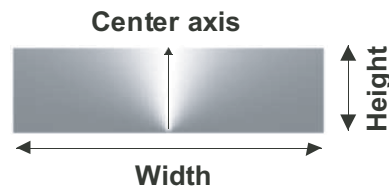


**Fig. 2** Angular alloy profile where the Indium concentration depends on the polar angle relative to the center axis of the QD. Light and dark grey-scale indicates high and low In content, respectively.

Here,  $E$  is the excitonic transition energy,  $E_0$  the zero-field energy,  $p_v$  and  $p_l$  are the intrinsic (vertical and lateral) dipole moments along the field that reflect the zero-field separation of the electron and hole wave function and  $\chi_v, \chi_l$  are the (vertical and lateral) polarizabilities.

**4.1 Vertical dipole moment as a function of the lateral electric field** Our calculations show that the change of the vertical dipole moment that follows from the response of the exciton to the vertical field for given lateral electric field depends very sensitively on the shape of the quantum dot. In fact, the vertical dipole moment increases with increasing lateral electric field for the obelisc shaped dots but decreases for the lens-shaped QD (Fig. 3). This is true irrespective of the type of alloy profile even though the effect is less pronounced for the radial profile due to the stronger lateral confinement of the hole. The physical origin of the pronounced lateral field dependence of the dipole moment may be understood as follows. The hole wave function is always located near the tip of the QD and thus basically moves along the surface of the dot when a lateral field is applied. The electron wave function, on the other hand, is more extended and remains delocalized within the entire QD up to fairly high values of the lateral field. Since the top part of the obelisc QD is flat, the center of mass of the hole stays at a constant height and moves along the surface with increasing lateral field. This effect alone would lead to a constant dipole

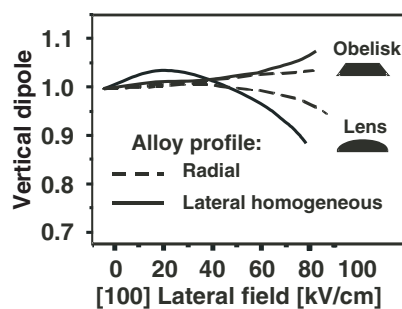


**Fig. 3** Ratio of the vertical excitonic dipole moment relative to its zero field value for the two classes of quantum dot shapes and alloy profiles, respectively, as a function of the lateral field.

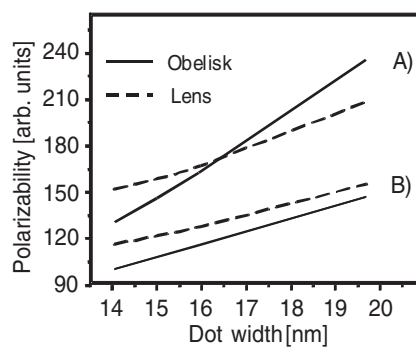


**Fig. 4** Predicted lateral polarizability shown as a function of the base width of the quantum dot for different shapes and alloy profiles. The polarizability is much larger for dots (A) with a laterally homogeneous alloy profile than for (B) dots with a radial profile since the latter provides a strong lateral confinement for the hole. For both alloy profiles, the results are shown for obelisc-shaped (full lines) as well as for lens-shaped quantum dots (dashed lines).

moment. However, the large strain at the edge of the obelisk deforms the confining potential in such a way that the hole gets partly localized outside the QD. This leads to an increase in the dipole moment. By contrast, a lens shaped QD possesses a curved surface that becomes thinner towards the edge so that the vertical distance between the centers of mass of hole and electron wave function necessarily decreases with increasing field. This explains qualitatively the results shown in Fig. 3. We note that fairly high lateral fields of more than 50 kV/cm are needed for observing a significant change in the dipole moment which may not be easy to realize experimentally.

**4.2 Lateral polarizability for different alloy profiles** The polarizability of the exciton in a lateral electric field is another sensitive measure of the alloy profile of the quantum dot that depends particularly on the base width of the QD (Fig. 4). In the case of the vertically linear alloy profile, one has a laterally homogeneous indium concentration. Not surprisingly, this yields a very large polarizability for both types of QD shapes. The radial alloy profile, on the other hand, leads to an inverted pyramid of indium content in the QD that in turn gives a strong lateral confinement of the hole. This effect reduces the polarizability drastically, typically by a factor of two compared to the linear alloy profile. Therefore, the alloy profile can be determined once the width of the quantum dot is known. The dots with a radial profile show a base width dependence of the polarizability that is very similar for both types of QD shapes. By contrast, QD with a laterally homogeneous profile possess a strong width dependence of the polarizability when they are obelisk-shaped but a weak one in the lens-shaped case. This is due to the fact that the curved surface of the lens QD enhances the lateral confinement which in turn limits the polarizability.

**5 Conclusion** We have shown that the shape and alloy composition of a self-assembled InGaAs quantum dot can be successfully predicted by analyzing the response of the neutral exciton to externally applied vertical and lateral electric fields. This extension of the Stark shift analysis [7] to both vertical and lateral directions provides important new insights into the electronic structure of quantum dots. Therefore, the combination of vertically and laterally applied electric fields is the ideal tool to determine uniquely the shape and the alloy profile of embedded InGaAs quantum dots.

**Acknowledgement** Financial support by the Deutsche Forschungsgemeinschaft and by the Office of Naval Research under Contract No. N00014-01-1-0242 is gratefully acknowledged.

## References

- [1] D. M. Bruls, J. W. A. M. Vugs, P. M. Koenraad et al., to be published.
- [2] N. Liu, J. Tersoff, O. Baklenov et al., *Phys. Rev. Lett.* **84**, 334 (2000).
- [3] X. Z. Liao, J. Zou, X. F. Duan, and D. J. H. Cockayne, *Phys. Rev. B* **58**, R4235 (1998).
- [4] I. Kegel, T. H. Metzger, A. Lorke et al., *Phys. Rev. B* **63**, 035318-1 (2001).
- [5] F. Findeis, M. Baier, E. Beham et al., *Appl. Phys. Lett.* **78**, 2958 (2001).
- [6] J. J. Finley, A. D. Ashmore, A. Lemaitre et al., *Phys. Rev. B* **63**, 073307-1 (2001).
- [7] P. W. Fry, D. J. Mowbray, I. E. Itskevich et al., *phys. stat. sol. (b)* **224**, 497 (2001).
- [8] G. Czajkowski, F. Bassani, and L. Silvestri, *phys. stat. sol. (a)* **188**, 1281 (2001).
- [9] R. J. Warburton, C. Schulhauser, D. Haft et al., *Phys. Rev. B* **65**, 113303/1 (2002).
- [10] J. El Khamkhami, E. Feddi, E. Assaid et al., *Phys. Low-Dimens. Struct.* **9**, 131 (2001).
- [11] J. Seufert, M. Obert, M. Scheibner et al., *Appl. Phys. Lett.* **79**, 1033 (2001).
- [12] W. H. Chang, T. M. Tsu, C. C. Huang et al., *Phys. Rev. B* **62**, 6959 (2000).
- [13] M. Pacheco and Z. Barticevic, *Phys. Rev. B* **64**, 033406/1 (2001).
- [14] A. J. Williamson, L. W. Wang, and A. Zunger, *Phys. Rev. B* **62**, 12963 (2000).
- [15] G. Klimeck, F. Oyafuso, R. C. Bowen et al., *Superlattices Microstruc.* **31**, 171 (2002).
- [16] S. Hackenbuchner, M. Sabathil, P. Vogl et al., *Physica B* **314**, 145 (2002).
- [17] O. Stier, M. Grundmann, and D. Bimberg, *Phys. Rev. B* **59**, 5688 (1999).
- [18] J. R. Downes, D. A. Faux, and E. P. O'Reilly, *J. Appl. Phys.* **81**, 6700 (1997).
- [19] J. Seufert, M. Obert, M. Scheibner, N. A. Gippius, G. Bacher, A. Forchel, T. Passow, K. Leonardi, and D. Hommel, *Appl. Phys. Lett.* **79**, 1033 (2001).